SHORT-LIVED RADIOISOTOPE INJECTION INTO THE SOLAR NEBULA: FIRST 3D CALCULATIONS OF SHOCK INTERACTIONS WITH ROTATING PRESOLAR CLOUD MODELS. Alan P. Boss & Sandra A. Keiser, DTM, Carnegie Institution (boss@dtm.ciw.edu).

The presence of live ^{60}Fe during the formation of chondrites [1,2] has long been seen as the strongest argument in favor of the injection of ^{60}Fe and other short-lived radioisotopes (SLRIs) into the presolar cloud [3] (or the solar nebula [4]) by a shock wave emanating from a Type II supernova (SNe) that synthesized the SLRIs. However, recent work has lowered the inferred initial abundances of ^{60}Fe [5] to values that are more consistent with the galactic background abundance rather than a nearby supernova [6]. This explanation might require the high levels of initial ^{26}Al found in chondrites to be derived from a Wolf-Rayet (WR) star wind, which is expected to be rich in ^{26}Al and poor in ^{60}Fe [6]. Scenarios have also been advanced for accounting for the inferred levels of both ^{60}Fe and ^{26}Al through supernova injection into giant molecular clouds [7,8,9], though abundance problems remain.

The presence of live ^{26}Al in refractory inclusions (e.g., CAIs) was the original motivation for the SNe trigger hypothesis. The fact that the FUN refractory inclusions show no evidence for live ^{26}Al, coupled with the significant ^{26}Al depletions found in some CAIs and refractory grains, implies that these refractory objects may have formed prior to the injection, mixing, and transport of ^{26}Al into the refractories-forming region of the solar nebula [10, 11, 12]. The ^{26}Al data alone, therefore, seem to require the late arrival of SLRIs derived from a SNe into the inner region of the solar nebula, as opposed to injection into a giant molecular cloud.

Detailed hydrodynamical modeling has shown that SNe shock waves are the preferred means for simultaneously achieving triggered collapse of the presolar cloud and injection of SLRIs carried by the shock wave [13]. WR star winds are likely to shred cloud cores rather than induce collapse [13]. These studies also showed that injection into a *rotating* cloud can increase injection efficiencies by as much as a factor of 10. However, the models [13] were restricted to axisymmetry (2D). Other previous models have studied shock wave interactions with fully 3D cloud cores [14]. However, these 3D clouds were not assumed to be rotating. Here we extend the modeling effort to consider rotating 3D target clouds.

The rotating presolar clouds are similar to those previously studied in 2D [13]: 2.2 $M_\odot$ cloud cores with radii of 0.053 pc, rotating with angular velocities of either $\Omega = 10^{-14}$ or 10^{-13} rad s^{-1}. The shock waves propagate along the rotation axis at speeds of $v_s = 20$ or 40 km s^{-1}, shock widths of $w_s = 3 \times 10^{-3}$ or 3×10^{-4} pc, and shock densities ranging from $\rho_s = 3.6 \times 10^{-19}$ to 2.1×10^{-17} g cm^{-3}. Most of the clouds were triggered into collapse. Several of the clouds with $\Omega = 10^{-13}$ collapsed and fragmented into multiple protostars.

The figures show the results for two models with $v_s = 40$, $w_s = 3 \times 10^{-4}$, and $\rho_s = 7.2 \times 10^{-18}$ in the previous units. Model H, with $\Omega = 10^{-13}$, formed a large ($\sim$ 500 AU radius) protostellar disk with spiral arms that might undergo fragmentation, while model L, with $\Omega = 10^{-14}$, formed a smaller diameter ($\sim$ 150 AU radius) protostellar disk with a single protostar. The injection efficiency f_i, defined [13,14] as the fraction of the incident shock wave material that is injected into the collapsing cloud core, was $f_i \sim 0.03$ for both models H and L, identical to f_i for the non-rotating-cloud version of this same model [14]. This differs from the expectations of the 2D models [13], where it was found that rotation could increase f_i by a factor as large as 10. However, the rotating 2D models studied only the standard shock ($\rho_s = 3.6 \times 10^{-20}$, $w_s = 3 \times 10^{-3}$), whereas models H and L considered denser, thinner shocks that are much more conducive to injection than the standard shock [13], so that the addition of rotation did not increase the injection efficiency further. Other shock assumptions can result in rotation leading to increased f_i, provided the shock is aligned with the rotation axis [13].

References: [1] Tachibana, S., et al. (2006), ApJ, *639*, L87. [2] Dauphas, N., & Chaussidon, M. (2011), AREPS, *39*, 351. [3] Boss, A. P. (1995), ApJ, *439*, 224. [4] Ouellette, N., et al. 2007, ApJ, *662*, 1268. [5] Telus, M., et al. (2012), MAPS, *47*, 2013. [6] Tang, H., & Dauphas, N. (2012), EPSL, *359-360*, 248. [7] Pan, L., et al. (2012), ApJ, *756*, 102. [8] Gounelle, M., & Meynet, G. (2012), A&A, *545*, A4. [9] Vasileiadis, A., et al. (2013), ApJL, *769*, L8. [10] Krot, A. N., et al. (2012), MAPS, *47*, 1948. [11] Kita, N. T., et al. (2013), MAPS, *48*, 1383. [12] Sahijpal, S., & Goswami, J. N. (1998), ApJL, *509*, L137. [13] Boss, A. P., & Keiser, S. A. (2013), ApJ, *770*, 51. [14] Boss, A. P., & Keiser, S. A. (2012), ApJL, *756*, L9.

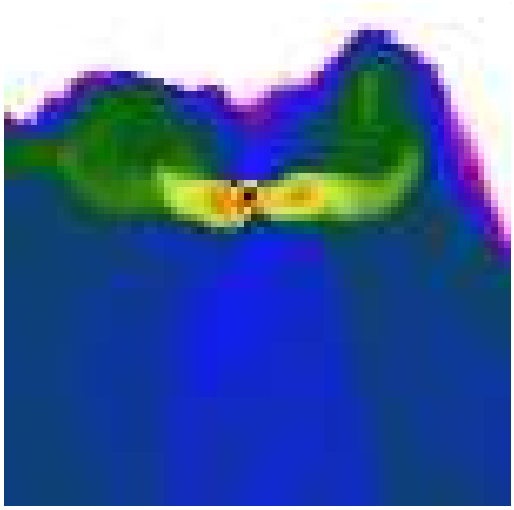

Fig. 1. Model H log density ($\rho_{max} \sim 10^{-11}$ g cm^{-3}) cross-section along rotation axis, showing edge-on disk. Region shown is 1333 AU across at 0.081 Myr.

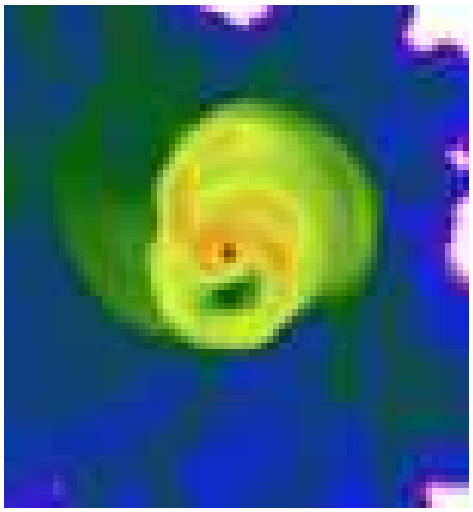

Fig. 2. Model H log density cross-section perpendicular to rotation axis, showing disk midplane. Region shown is 1333 AU across at 0.081 Myr.

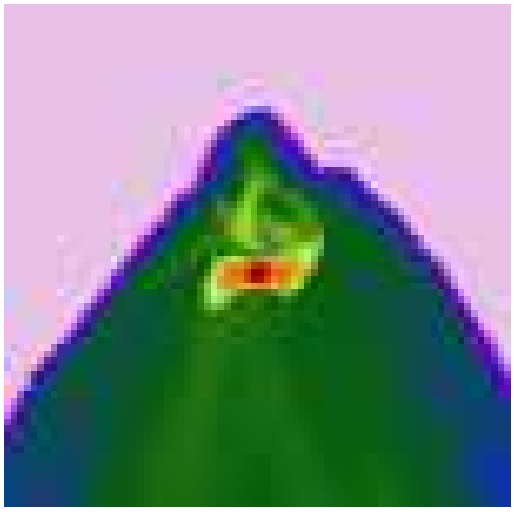

Fig. 3. Model L log density ($\rho_{max} \sim 10^{-11}$ g cm^{-3}), plotted as in Fig. 1 (1333 AU across) at 0.078 Myr. Disk radius is $\sim$ 150 AU.

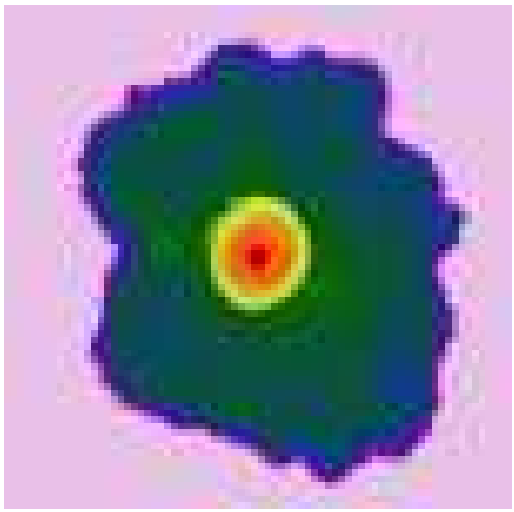

Fig. 4. Model L log density, plotted as in Fig. 2 (1333 AU across) at 0.078 Myr. No spiral arms are evident in this smaller disk at this phase.